摘 要

$Cu_{2.9}Mn_{0.1}Al$ 合金 (Cu-25.0at% Al-2.5at% Mn ; Cu-12.4wt % Al-2.5wt% Mn)在淬火狀態下的顯微組織為$D0_3$相＋γ_1' 麻田散體。$D0_3$相是在淬火過程中經由β → B2 → $D0_3$兩階段連續的有序-無序相變化形成，β→B2 以及B2→$D0_3$相變化過程分別產生了a/4<111>以及a/2<100>反向晶界。淬火後的$Cu_{2.9}Mn_{0.1}Al$合金經由 150℃ 到 750℃ 的時效其相變化順序為 ($D0_3$＋γ_1') → ($D0_3$＋γ_1'＋γ_2) → ($D0_3$＋β_1'＋γ_2) →(B2＋β_1'＋γ_2) → β相，其中β_1'(18R)麻田散體的形成是因為γ_2析出造成基地成分的改變以及內應力升高的緣故。

比較過去的研究，在不施加外力的情況下，β_1'(18R)麻田散體由γ_1'(2H)麻田散體轉變而來，是第一次在Cu-Al-Mn合金中被發現。當時效溫度升到 400℃ 的時候我們可以看到 γ-brass析出物經長時間時效由圓形變成長條形。另外，當時效溫度升到 550℃ 的時候經長時間時效，可以看到γ-brass析出物量增加的情況下，β_1'麻田散體量相對減少了。值得一提的是，在x＝0.1 的$Cu_{3-x}Mn_xAl$ 合金中不會有L-J相存在，此與之前在x≧0.2 的$Cu_{3-x}Mn_xAl$合金中所觀察到的不同。

Abstract

The as-quenched microstructure of the $Cu_{2.9}Mn_{0.1}Al$ alloy (Cu-25.0at% Al-2.5at% Mn ; Cu-12.4wt% Al-2.5wt% Mn)was a mixture of ($D0_3 + \gamma_1'$(2H)martensite). The $D0_3$ phase was formed by the $\beta \rightarrow B2 \rightarrow D0_3$ continuous two-stage order-disorder transition during quenching. The $\beta \rightarrow B2$ and $B2 \rightarrow D0_3$ transitions produced a/4<111> and a/2<100> APBs, respectively. When the as-quenched $Cu_{2.9}Mn_{0.1}Al$ alloy was aged at temperatures ranging from 150℃ to 750℃，the phase transition sequence was found to be $(D0_3 + \gamma_1') \rightarrow (D0_3 + \gamma_1' + \gamma_2) \rightarrow (D0_3 + \beta_1' + \gamma_2) \rightarrow (B2 + \beta_1' + \gamma_2) \rightarrow \beta$ where the β_1'(18R) martensite was transformed due to the chemical composition change and increase of internal stress by γ_2 precipitation.

Compared with previous studies, it is found that the β_1' martensite resulting from γ_1' martensite without applied stress is first observed in the $Cu_{3-x}Mn_xAl$ alloys. In addition, when the

as-quenched alloy was aged at 400℃, the original spherical γ-brass precipitate would change to plate-like. Moreover, the amount of γ-brass precipitate was increased and that of β_1' martensite was decreased during prolonged aging at 550℃. Finally, it is worthwhile to note that no L-J phase was observed in the present alloy ($x = 0.1$ in $Cu_{3-x}Mn_xAl$ alloys). This is quite different with that observed by previous workers in the $Cu_{3-x}Mn_xAl$ alloys with $x \geqq 0.2$.

Contents

.

List of Tables

List of Figures

Introduction

Phase transformations in $Cu_{3-x}Mn_xAl$ alloys have been extensively studied by many researchers before[1-6]. Based on those studies, the $Cu_{3-x}Mn_xAl$ phase diagram with $0.2 \leqq X \leqq 1$ was established by M. Bouchard et al. and R. Kainuma et al., respectively. These phase diagrams are shown in Figure 1 and 2. According to their phase diagrams, it is seen that when the $Cu_{3-x}Mn_xAl$ alloy with $0.2 \leqq X \leqq 1$ was solution heat-treated in single β phase (A2; disordered *bcc*) region and then quenched rapidly, a $\beta \rightarrow B2 \rightarrow D0_3 + L2_1$would occur through an order-disorder transition and a spinodal decomposition[1,2]. It means that the as-quenched microstructure of the $Cu_{3-x}Mn_xAl$ alloy with $0.2 \leqq X \leqq 1$ was a mixture of ($D0_3 + L2_1$) phases. While the as-quenched microstructure of the $Cu_{3-x}Mn_xAl$ alloy with $x = 1$ became a single $L2_1$ phase. The $L2_1$ phase was formed through a $\beta \rightarrow B2 \rightarrow L2_1$ transition during quenching. The $L2_1$ structure is very similar to the $D0_3$ structure. The only difference between them is that the manganese atoms replaced the copper atoms at a

specific lattice site with eight nearest copper atoms in the $D0_3$ structure so as to form a stoichiometric composition of Cu_2MnAl[3], as shown in Figure 3[1].

When the as-quenched $Cu_{3-x}Mn_xAl$ alloys were aged at 700 ℃ or below for different times, α-Mn, β-Mn, T_3-Cu_3Mn_2Al and γ_2-Cu_9Al_4 would be formed within the matrix [2,5-11,29]. The α-Mn has a cubic structure with lattice parameter a=0.891nm [29]. The β-Mn has an A13(simple cubic)structure with lattice parameter a=0.641nm. The T_3 phase has a C15 structure (ordered *fcc*) with lattice parameter a=0.691nm. The γ-brass has a $D8_3$ (ordered complex body-centered cubic) structure with lattice parameter a=0.872 nm[12-15]. The orientation relationship between the γ-brass and the matrix is cubic to cubic[16,17].

To date, most of the studies are focused on the $Cu_{3-x}Mn_xAl$ alloy with $0.2 \leqq X \leqq 1$. Little information concerning the phase transformation in the $Cu_{3-x}Mn_xAl$ alloy with $X < 0.2$ has been provided. Therefore, the purpose of the present study is to examine the phase transformation of the $Cu_{2.9}Mn_{0.1}Al$ alloy by

using transmission electron microscopy and energy dispersive X-ray spectrometer analyses (EDS).

Experimental Procedure

(A) Alloy Preparation

The $Cu_{2.9}Mn_{0.1}Al$ alloy was prepared by melting the elements as 99.99 pct. copper, 99.99 pct. aluminum and 99.99 pct. manganese together in an induction furnace. The melt was chill cast into a $30 \times 50 \times 200$-mm copper mold and subsequently homogenized at 910℃ for 72 hours under a protective argon atmosphere. After homogenization, the ingot was cut and then hot-rolled to a thickness about 2.0 mm. Finally, the specimens were solution heat-treated at 910℃ for 1 hour and rapidly quenched into iced brine (NaCl). The aging processes were performed at the temperatures ranging from 100℃ to 750℃ in a vacuum furnace and then also quenched into iced brine rapidly .

(B) Transmission Electron Microscopy (TEM)

The electron microscopic specimen was first mechanically grinded and polished into thin foil and then chemically polished by means of a double jet electro-polisher with the

electrolyte of 70% methanol and 30% nitric acid. The polishing temperature was kept in the range from -30℃ to -20℃ and the current density was kept in the range from 3.0 $\times 10^4$ to 4.0 $\times 10^4$ A/m^2. Electron microscopy observations were carried out by a JEOL-2000FX scanning transmission electron microscope (STEM) operating at 200kV. This microscope was equipped with a Link ISIS 300 energy-dispersive X-ray spectrometer (EDS) for chemical analysis. Quantitative analyses of elemental concentrations for Cu, Al and Mn were made with the aid of a Cliff-Lorimer ratio Thin Section method.

(C) Optical Microscopy (OM) / Scanning Electron Microscopy (SEM)

The preparations of OM and SEM specimens are as the following procedures: Firstly, the surface of the sample sheets was modified by mechanical grinding and polishing. Secondly, the surface-modified sheets were etched in the solution of 80% methanol and 20% nitric acid until the

appearance of grain boundaries. Thirdly, while the etching process is finished washing the surface of the sheets right away in quantities of flowing water. Finally, drying up the sheets with nonfat cotton and then heating them.

Results and Discussion

Figure 4 is a typical EDS spectrum of the alloy in the as-quenched condition. The quantitative analysis of Energy Dispersive Spectrometer(EDS) indicated that the composition was Cu-2.5wt%Mn-12.4wt%Al (Cu-2.5at%Mn-25.0at%Al). Figure 5 (a) is an optical micrograph of the as-quenched alloy revealing that a high density of plate-like phase was formed within the matrix. Figure 5 (b) is a bright-field(BF) electron micrograph of the as-quenched alloy indicating the presence of the plate-like phase. Figures 5(c) and 5(d) are two selected-area diffraction patterns (SADPs) taken from a plate-like phase and its surrounding matrix. In these SADPs, it is seen that besides the reflection spots corresponding to $D0_3$ phase, some extra spots could be detected owing to the presence of the plate-like phase. Compared with previous studies[18-21], it is found that the extra spots could be indexed as γ_1' martensite with internal twins. The γ_1' martensite has an orthorhombic structure with lattice parameters a = 0.455 nm, b = 0.502 nm and c = 0.429 nm[22]. Figure 5(e) is a (111) $D0_3$ dark- field (DF) electron

micrograph of the as-quenched alloy clearly showing the presence of the fine $D0_3$ domains with a/2<100> anti-phase boundaries (APBs). Figure 5(f) is a (200) $D0_3$ DF electron micrograph revealing the presence of the small B2 domains with a/4<111> APBs. Since, the sizes of both $D0_3$ and B2 domains are very small. Consequently, it is deduced that the $D0_3$ phase in the as-quenched alloy was formed by a $\beta \rightarrow B2 \rightarrow D0_3$ continuous ordering transition during quenching[1-2]. Figure 5(g) is a $(1\,\bar{2}\,1)$ γ_1' DF electron micrograph, clearly showing the presence of the plate-like γ_1' martenstie. Based on above observations, it is concluded that the as-quenched microstructure of the $Cu_{2.9}Mn_{0.1}Al$ alloy is a mixture of ($D0_3 + \gamma_1'$ martenstie), where the $D0_3$ phase was formed by a $\beta \rightarrow B2 \rightarrow D0_3$ continuous ordering transition during quenching.

Figures 6(a) and 6(b) are an optical micrograph and a BF electron micrograph of the $Cu_{2.9}Mn_{0.1}Al$ alloy aged at 150℃ for 100 hours and then quenched, respectively. Obviously, the morphology is similar to that observed in Figures 4(a) and 4(b). Moreover, electron diffraction demonstrated that the micro-

structure of the $Cu_{2.9}Mn_{0.1}Al$ alloy aged at 150℃ for 100 hours was still the mixture of ($D0_3$ + γ_1' martenstie). Figure 6(c) is a (111) $D0_3$ DF revealing that the size of $D0_3$ domains grew considerably during aging. It means that the microstructure of the matrix at 150℃ was $D0_3$ phase.

Figure 7(a) is an optical micrograph of the $Cu_{2.9}Mn_{0.1}Al$ alloy aged at 400℃ for 1 hour and then quenched. In this figure, it is clear that a high density of fine precipitates was observed within the matrix or on the grain boundaries and no evidence of the γ_1' martensite could be detected. Figure 7(b) is an optical micrograph of the alloy aged at 400℃ for 100 hours. Evidently, some plate-like precipitate started to appear within the matrix. Figure 7(c) is a BF electron micrograph of the alloy aged at 400 ℃ for 100 hours. Figures 7(d) and 7(e) are two SADPs taken from the e precipitate marked as “R” in Figure 7(c). According to the camera length and the measurements of angles as well as d-spacings of the diffraction spots, the crystal structure of the precipitate was determined to be an ordered body-centered cubic structure with lattice parameter a = 0.872 nm, which is

consistent with that of the γ_2 phase[1,8,23]. Figure 7(f) through 7(h) are three SADPs taken from an area marked as "M" in Figure 7(c). When compared with previous studies in Cu-based shape memory alloys[24-27], it is found that the positions and streak behaviors of the reflection spots are the same as those of the β_1' martensite. The β_1' martensite has a monoclinic structure with lattice parameters a = 0.446 nm, b = 0.529 nm, c = 3.838 nm and β = 89.4°, respectively[24]. Figure 7(i) is a (001) γ_2 DF electron micrograph, indicating the presence of the γ_2 precipitate.

Figures 8(a) and 8(b) are two optical micrographs of the $Cu_{2.9}Mn_{0.1}Al$ alloy aged at 550℃ for 1 hour and 100 hours, respectively. Compared with these two micrographs, it is found that with increasing the aging time, the amount of γ-brass precipitate increased but that of the β_1' martensite decreased. Figure 8(c) is a BF electron micrograph of Figure 8(b). Figure 8(d) is a SADP of the β_1' martensite. The zone axis is [010]. It is worthwhile to note that the streak behaviors become weaker.

Figure 9(a) is an optical micrograph of the $Cu_{2.9}Mn_{0.1}Al$

alloy aged at 750℃ for 2 hours revealing that the microstructure is similar to that observed in the as-quenched alloy. Figure 9(b) is a BF electron micrograph, showing the existence of the plate-like γ_1' martensite. Figure 9(c) is a (111) $D0_3$ DF electron micrograph of the same area as Figure 9(b), revealing the presence of the $D0_3$ domains with a/2<100> APBs. Figure 9(d) is a (200) $D0_3$ DF electron micrograph of the same area as Figure 9(b), revealing the presence of the B2 domains with a/4<111> APBs. This result indicates that the microstructure existing at 750℃ or above is a single disordered β phase.

Based on the above experimental results, it is concluded that with increasing the aging temperature from 100℃ to 750℃, the phase transition sequence in the present alloy is $(D0_3 + \gamma_1') \rightarrow (D0_3 + \gamma_2 + \gamma_1') \rightarrow (D0_3 + \gamma_2 + \beta_1') \rightarrow (B2 + \gamma_2 + \beta_1') \rightarrow$ single β . The first transition occurs between 150℃ and 250℃, the second between 250℃ and 400℃, the third between 560℃ and 650℃ and the fourth between 650℃ and 750℃, respectively.

A change of the martensite type from γ_1' to β_1' after γ_2

precipitation was noted, which is consistent with the existing phase diagram of Cu-Al binary alloys shown in Figure 10. The γ_2 precipitate is an aluminum-rich phase(Cu-16.0wt%Al-1.9wt%Mn[7]) compared with the present alloy. Thus, the formation of γ_2 precipitate cause a decrease of aluminum content and an increase of manganese content in the matrix. The composition change of this study during aging is shown in Table 1. It is seen that the change of manganese content is a little. Thus, the change of manganese content can be neglected. According to the change of aluminum content of the present alloy, it is reasonable that the martensite type is changed from γ_1' to β_1'. Figure 11 is a diagram of types of martensite with factors of temperature and stress. It is seen that higher stress lead to 18R(β_1') martensite. Based on above discussion, it is suggested that the change of martensite type from γ_1' to β_1' in the present study is due to the chemical composition change and increase of internal stress by γ_2 precipitation.

Finally, it is worthwhile to note that no L-J phase could be observed in the $Cu_{2.9}Mn_{0.1}Al$ alloy. According to previous

studies on the as-quenched microstructure of $Cu_{3-x}Mn_xAl$ alloys with $x \geqq 0.2$[18], it is found that the L-J phase was always observed. This result suggest that since the L-J phase is a manganese-rich phase (Cu-17.52at%Al- 15.3at%Mn) [23], the manganese content in the present alloy was too low to observe the presence of the L-J phase.

Conclusions

(1) Phase transformations in the $Cu_{2.9}Mn_{0.1}Al$ alloy have been examined by using transmission electron microscopy. In the as-quenched condition, the microstructure of the $Cu_{2.9}Mn_{0.1}Al$ alloy was a mixture of ($D0_3 + \gamma_1'$ martensite). The $D0_3$ phase was formed through the $\beta \rightarrow B2 \rightarrow D0_3$ ordering transition during quenching.

(2) When the as-quenched $Cu_{2.9}Mn_{0.1}Al$ alloy was aged at temperatures ranging from 150℃ to 750℃, the phase transition sequence was formed to be $(D0_3 + \gamma_1') \rightarrow (D0_3 + \gamma_2 + \gamma_1') \rightarrow (D0_3 + \gamma_2 + \beta_1') \rightarrow (B2 + \gamma_2 + \beta_1') \rightarrow \beta$. The first transition occurs between 150℃ and 250℃, the second between 250℃ and 400℃, the third between 560℃ and 650℃ and the fourth between 650℃ and 750℃, respectively.

(3) It is suggested that the change of martensite type from γ_1' to β_1' in the present study is due to the chemical composition change and increase of internal stress by γ_2 precipitation. The γ_2 precipitation cause a decrease of aluminum content

and an increase of internal stress in the matrix.

References

[1]M. Bouchard and G. Thomas : Acta Metall., Vol. 23, pp.1485-1500 (1975).

[2]R. Kainuma, N. Satoh, X.J. Liu, I. Ohunuma and K. Ishida : J. Alloys and Compounds, 266 ,pp.191-200 (1998).

[3]Ye.G. Nesterenko and I.A. Osipenko: Fiz. Metal. Metalloved., 36, 1212(1973).

[4]S. C. Jeng and T. F. Liu: Metallurgical and Materials Transactions A, Vol.26A, pp.1353-1365(1995).

[5]D. R. F. West and D. Lloyd Thomas: Journal of the Institute of Metals Vol.85 pp.97-104(1956)

[6]J. Soltys, M. Stefaniak and J. Holender: Philosophical Magazines B, Vol.49, No.2 pp.151-158(1984)

[7]J. Dutkiewicz, J. Pons and E. Cesari: Materials Science and Engineering A158 pp.119-128(1992)

[8]J. Miettinen: Calphad, Vol.27, No.1, pp.103-114(2003)

[9]M. O. Prado and A. Tolley: Materials Science and Engineering A273-275 pp.590-594(1999)

[10]K. C. Chu and T. F. Liu: Metall. Trans. A.,30, 1705(1999)

[11]Eduard Obradó, Carlos Frontera, Lluís Mañosa and Antoni Planes: Physical Review B, Vol.58, No.21, pp.14245-14255 (1998)

[12]J. I. Pérez-Landazábal, V. Recarte and V. Sánchez-Alarcos: J. Phys.: Condens. Matter 17, pp.4223-4236(2005)

[13]X. J. Liu, I. Ohnuma, R. Kainuma and K. Ishida: Journal of Alloys and Compounds 264, pp.201-208(1998)

[14]M. A. Dvorack, N. Kuwano, S. Polat, H. Chen and C. M. Wayman: Scripta Metall., Vol.17, pp.1333-1336(1983)

[15]J. Singh, H. Chen and C. M. Wayman: Scripta Metall., Vol.19, pp.887-890(1985)

[16]R. Kozubski and J. Soltys: Journal of Materials Science , 18, 1689(1983)

[17]J. Pons, E. Cesari: Materials Structure, Vol.6, No.2, pp.115-119(1999)

[18]S. Y. Yang and T. F. Liu: Materials Chemistry and Physics, 98, pp.389-394(2006)

[19]C. H. Chen and T. F. Liu: Materials Chemistry and Physics, 78, pp.464-473(2002)

[20]C. H. Chen, C. C. Yang and T. F. Liu: Materials Science and Engineering A354, pp.377-386(2003)

[21]C. H. Chen and T. F. Liu: Scripta Materialia, Vol.47, pp.515 -520(2002)

[22]I. R. Bubley, Yu. N. Koval, P. V. Titov: Scripta Materialia, Vol.41, No.6, pp.637-641(1999)

[23]S. Y. Yang and T. F. Liu: Scripta Materialia, 54, pp.931-935 (2006)

[24]Renhui Wang, Jianian Gui, Xiaomei Chen, Shusong Tan: Acta Materialia, 50, pp.1835-1847(2002)

[25]H. Y. Peng, Y. D. Yu and D. X. Li: Acta Materialia, Vol.45, No.12, pp.5153-5161(1997)

[26]D. Shi, J. Gui, S.S. Tan, R. Wang: Materials Science and Engineering B56, pp.31-36(1998)

[27]Y. J. Bai, X. G. Xu, Y. X. Liu, L. M. Xiao, G. L. Geng: Materials Science and Engineering A334, pp.49-52(2002)

[28]J. van Humbeeck et al.: Trans. JIM 28, 383(1987)

[29]W. Williams, Jr. and J. L. Stanford: Journal of Magnetism and Magnetic Materials 1 pp.271-285(1976)

Table 1 Chemical compositions of the phases revealed by and Energy Dispersive Spectrometer(EDS)

Heat Treatment	Phases	Chemical Composition (at%) Cu	Al	Mn
As-quenched	$D0_3+\gamma_1'$ martensite	72.5	25.0	2.5
250℃ aging 1.5hr	γ-brass	71.44	27.55	1.01
400℃ aging 1 hr	γ-brass	70.58	28.36	1.06
	β_1' martensite	73.69	23.72	2.59
510℃ aging 1 hr	γ-brass	70.28	28.47	1.25
	β_1' martensite	74.22	23.14	2.64
560℃ aging 100 hrs	γ-brass	62.68	35.39	1.93
	β_1' martensite	75.05	22.24	2.71

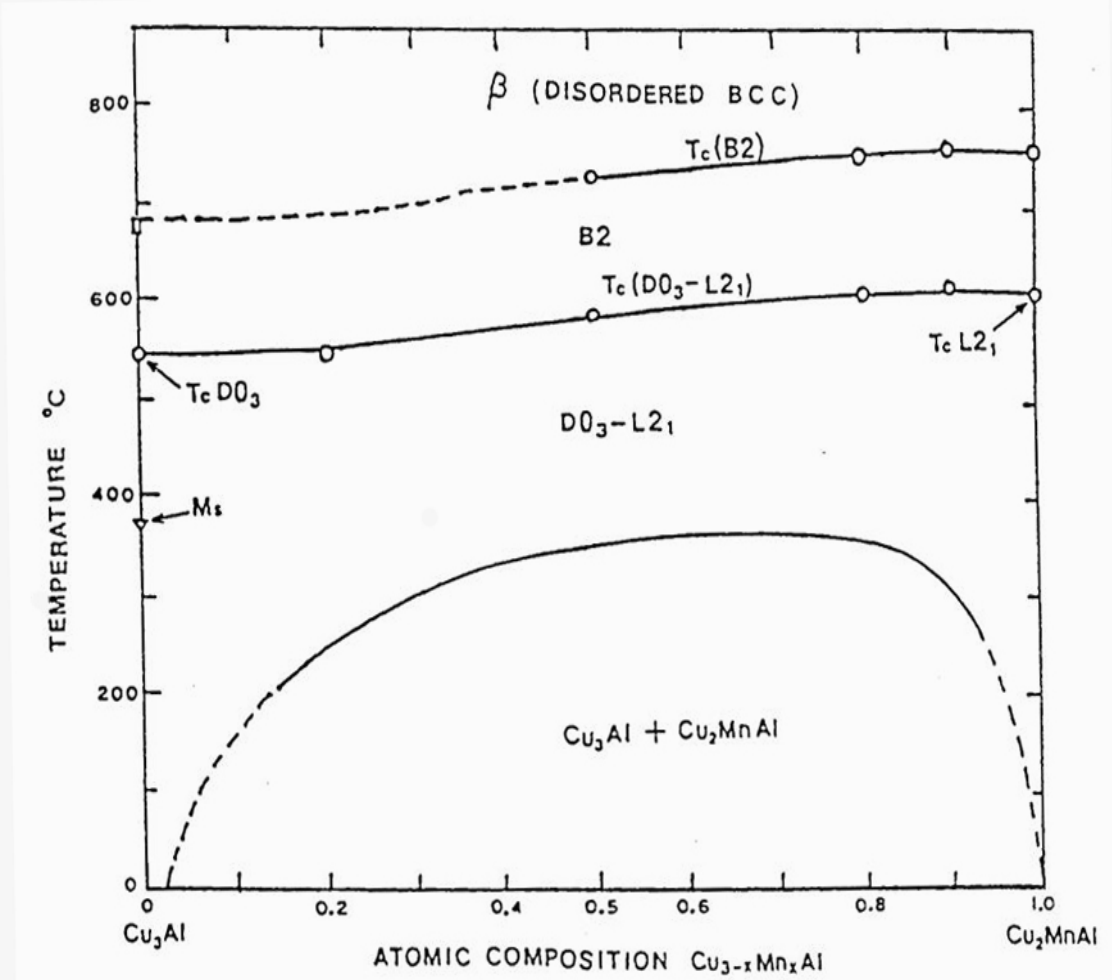

Fig. 1 A schematic drawing of the ordering temperatures Tc(B2) and Tc($D0_3$+$L2_1$) and the miscibility gap of the $Cu_{3-x}Mn_xAl$ alloy established by M. Bouchard and G. Thomas.

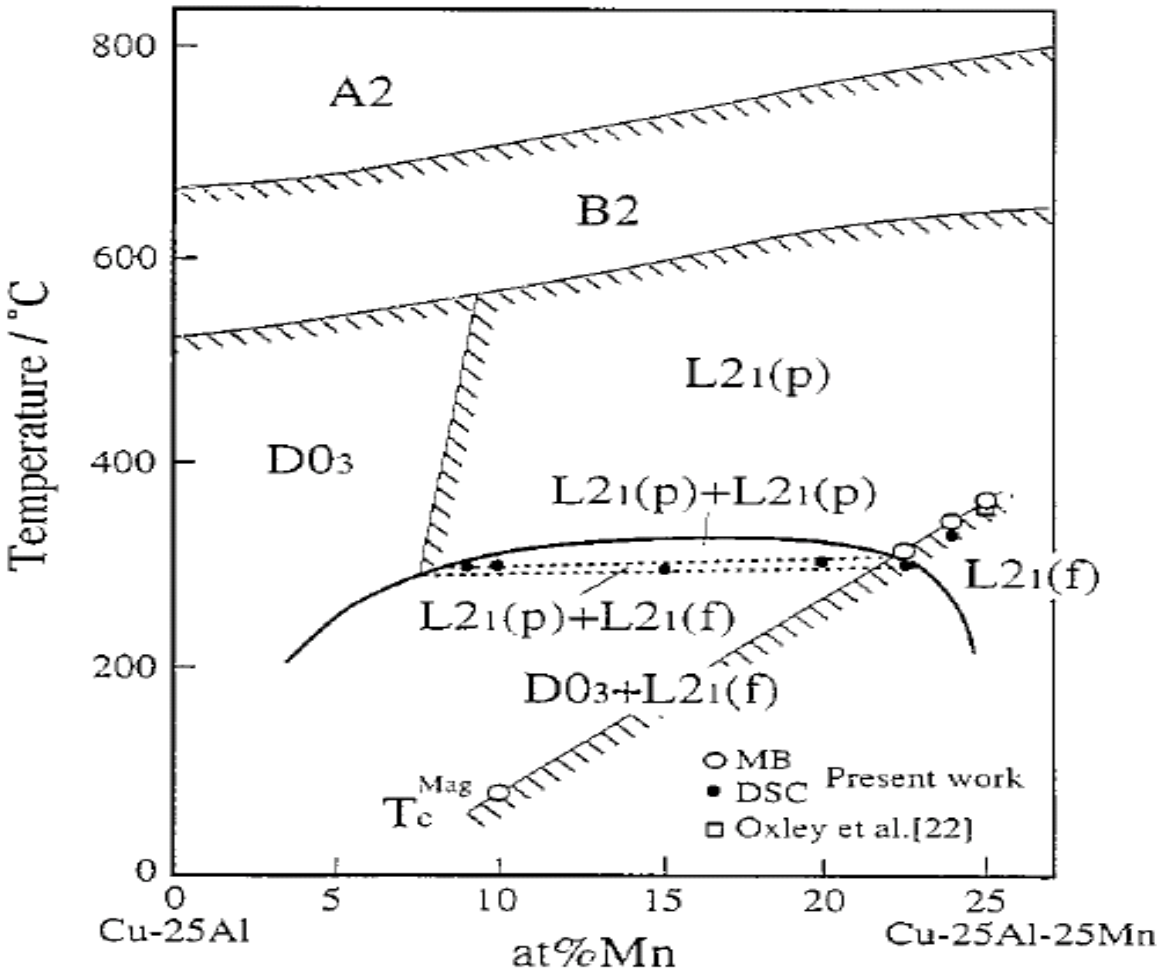

Fig. 2 A phase diagram established by R. Kainuma, N. Satoh, X.J. Liu, I. Ohunuma and K. Ishida.

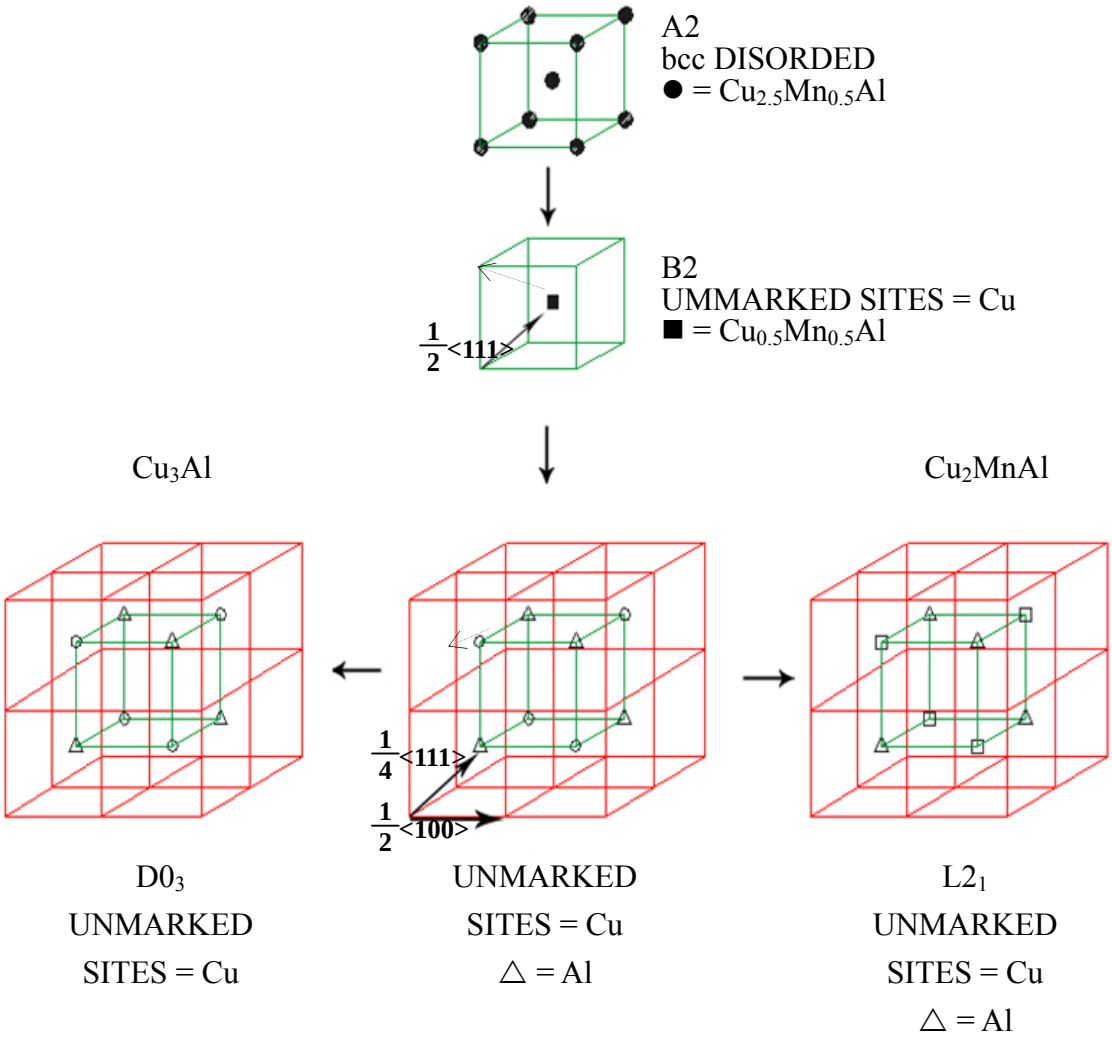

Fig. 3 Schematic representation of the ordering sequence of the quenched $Cu_{2.5}Mn_{0.5}Al$ alloy (vertically) and its isothermal decomposition (horizontally).

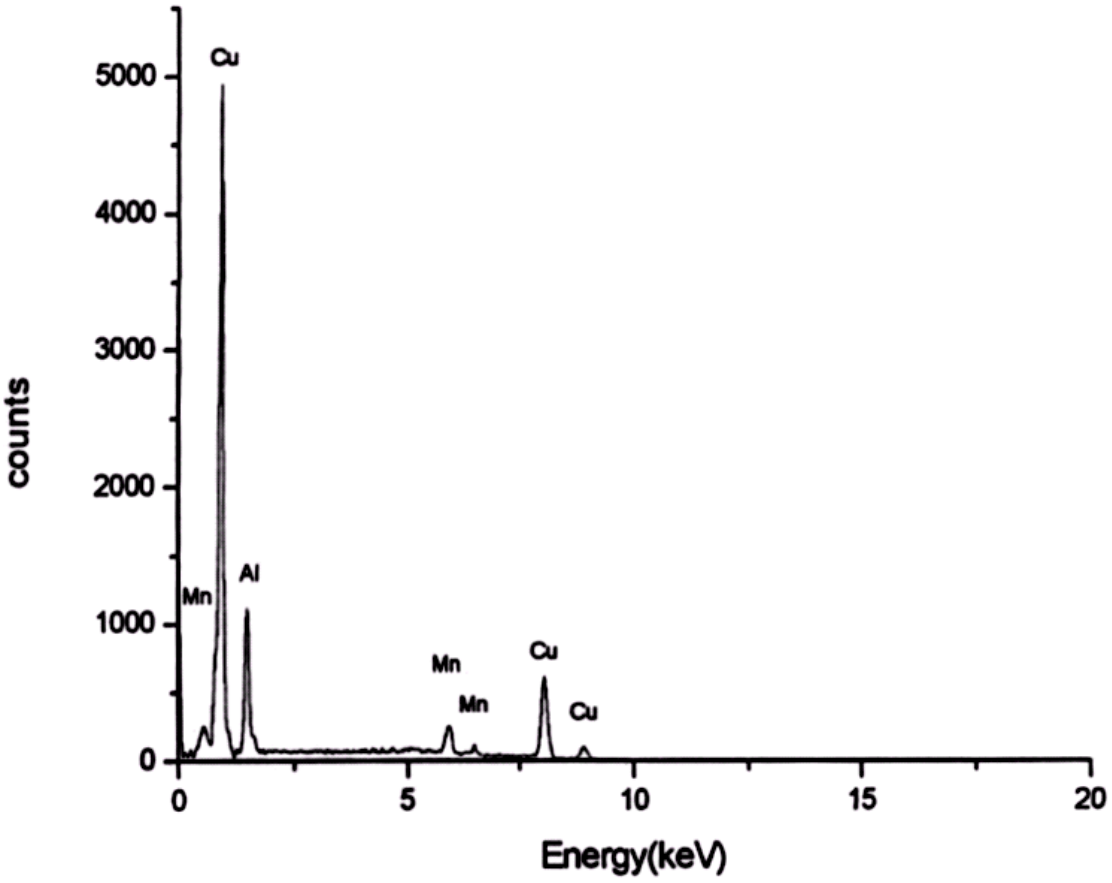

Fig. 4 A typical EDS spectrum of the as-quenched $Cu_{2.9}Mn_{0.1}Al$ alloy.

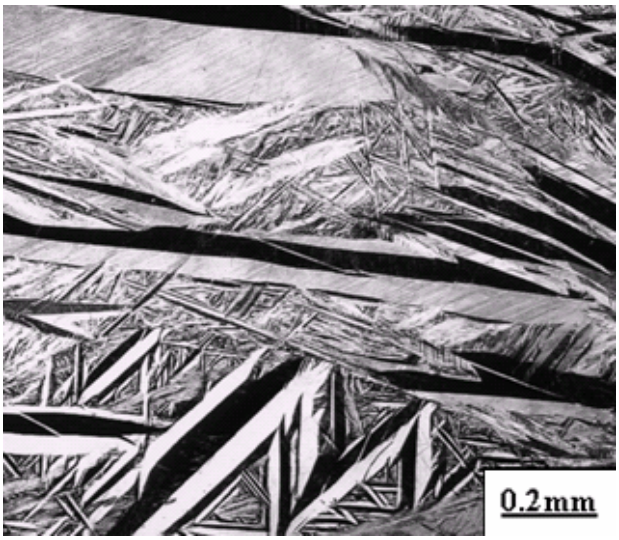

Fig. 5(a)

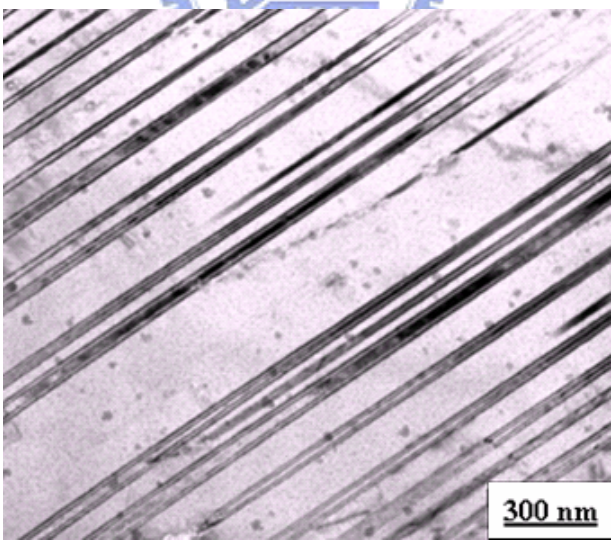

Fig. 5(b)

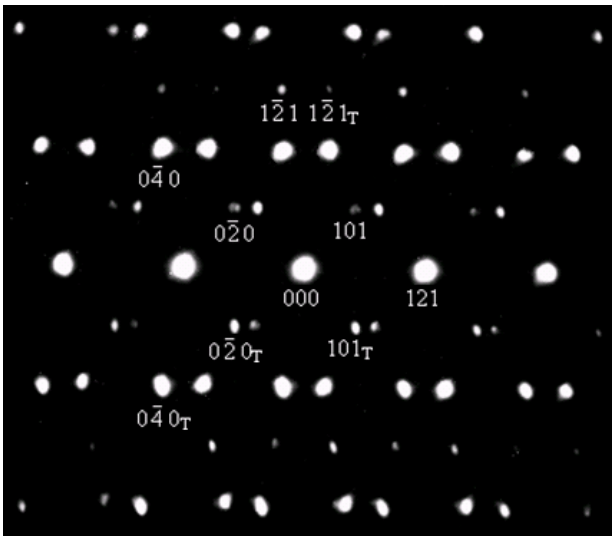
$1\bar{2}1\ 1\bar{2}1_T$
$0\bar{4}0$
$0\bar{2}0$
101
000
121
$0\bar{2}0_T$
101_T
$0\bar{4}0_T$

Fig. 5(c)

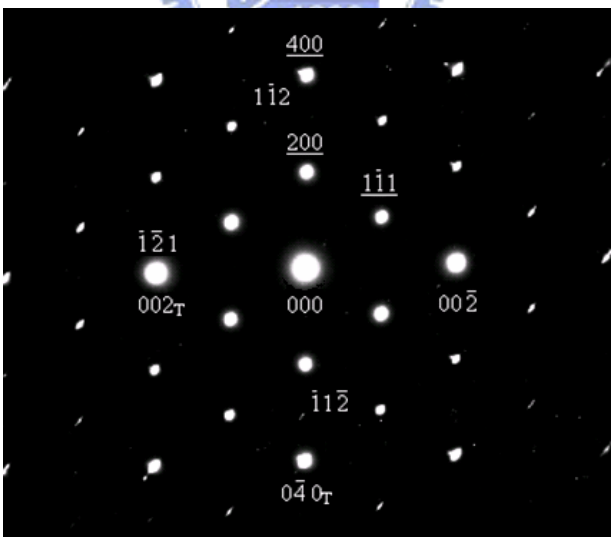
400
$1\bar{1}2$
200
$1\bar{1}1$
$\bar{1}\bar{2}1$
002_T
000
$00\bar{2}$
$\bar{1}1\bar{2}$
$0\bar{4}0_T$

Fig. 5(d)

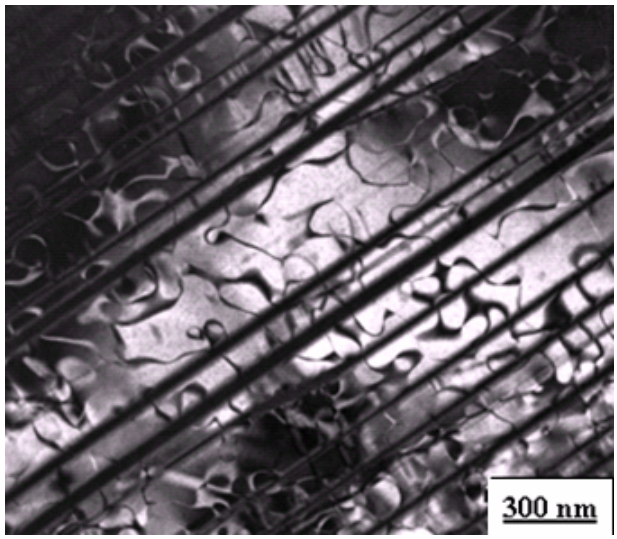

Fig. 5(e)

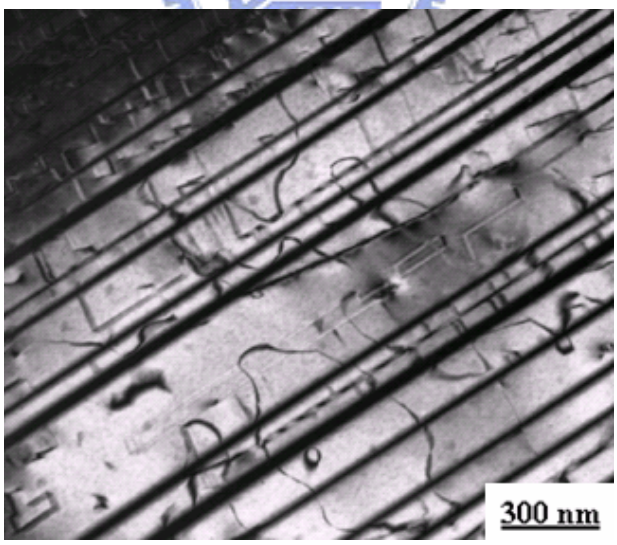

Fig. 5(f)

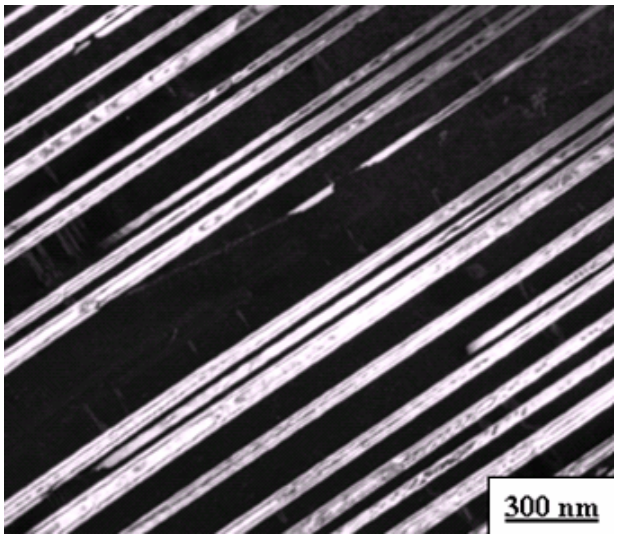

Fig. 5(g)

Fig. 5 (a) Optical micrograph. (b)-(g) Electron micrographs of the as-quenched $Cu_{2.9}Mn_{0.1}Al$ alloy: (b) BF, (c) and (d) two SADPs. The zone axes of the $D0_3$ phase, γ_1' martensite and internal twin are (b) [001], $[10\bar{1}]$ and $[\bar{1}01]$, (c) [011], $[1\bar{1}\bar{1}]$ and $[\bar{1}00]$, respectively. ($\underline{hkl}$=$D0_3$ phase, hkl=γ_1' martensite, hkl_T= internal twin). (d) and (e) (111) and (200) $D0_3$ DF, respectively. (g) $(1\bar{2}1)$ γ_1' DF.

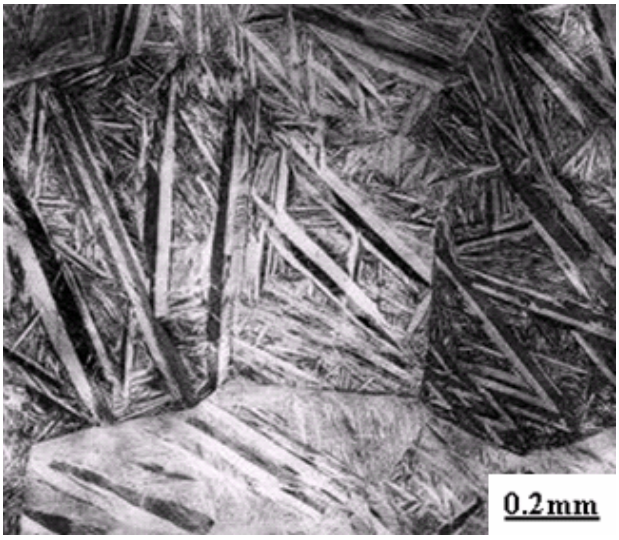

Fig. 6 (a)

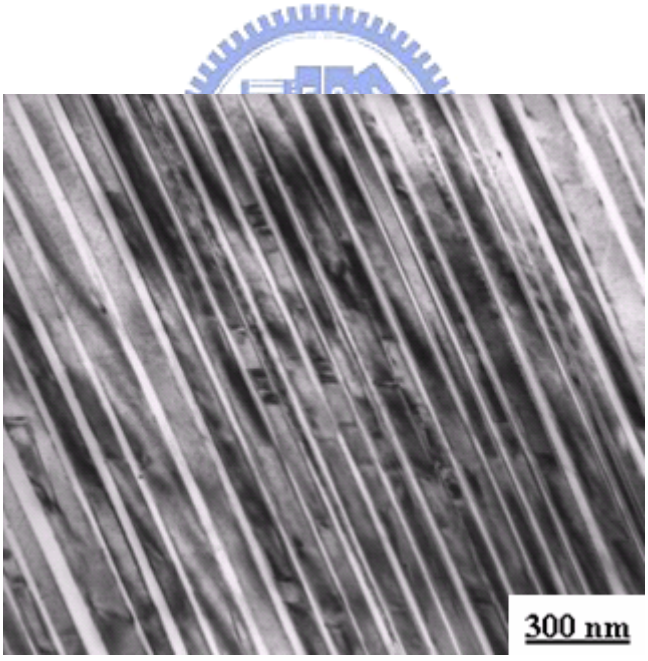

Fig. 6 (b)

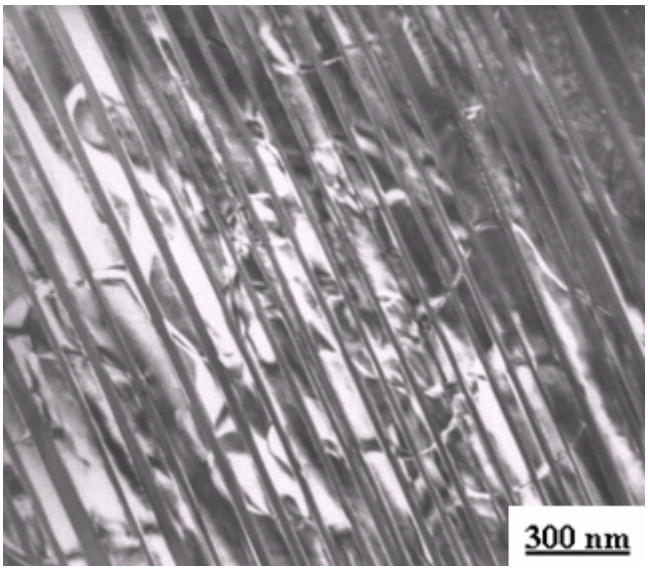

Fig. 6 (c)

Fig. 6 (a) Optical micrograph. (b)-(c) Electron micrographs of $Cu_{2.9}Mn_{0.1}Al$ alloy aged at 150℃ for 100 hours. (b)BF (c) (111) $D0_3$ DF.

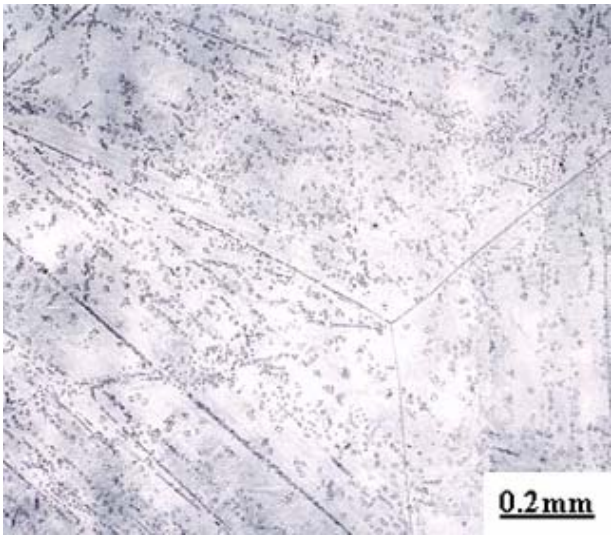

Fig. 7 (a)

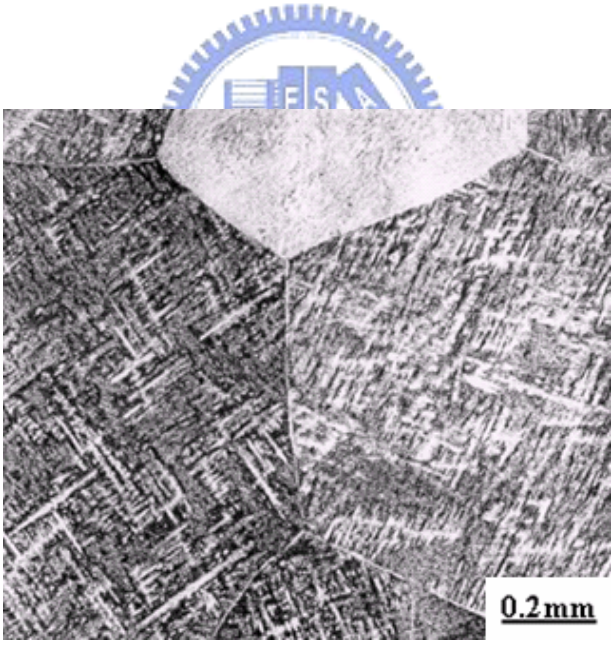

Fig. 7 (b)

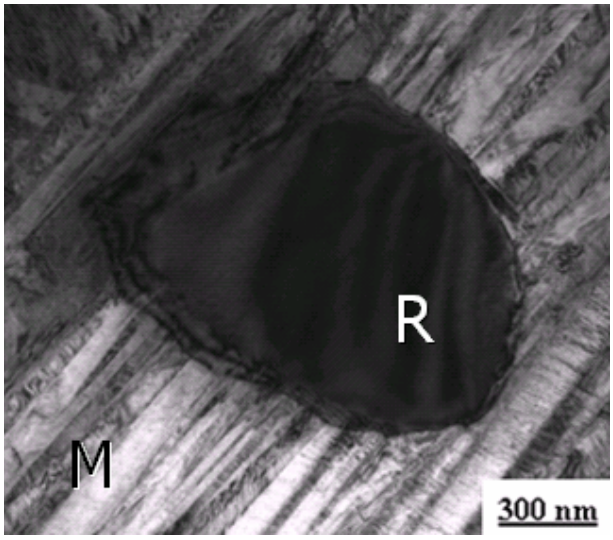

Fig. 7 (c)

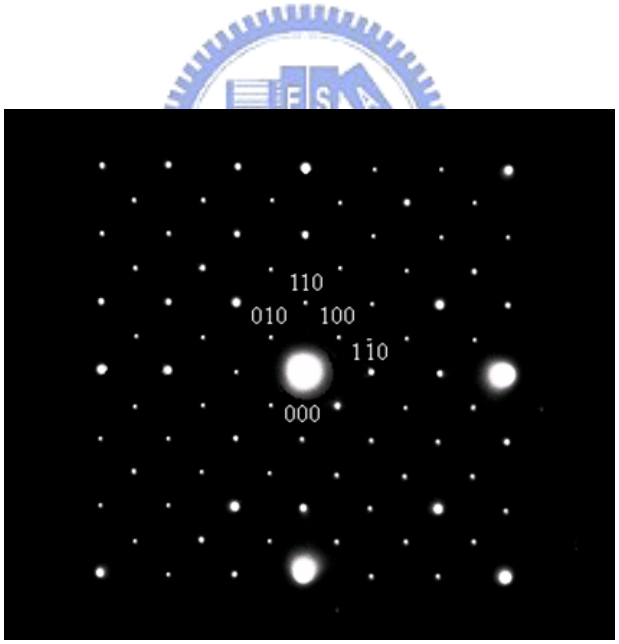

Fig. 7 (d)

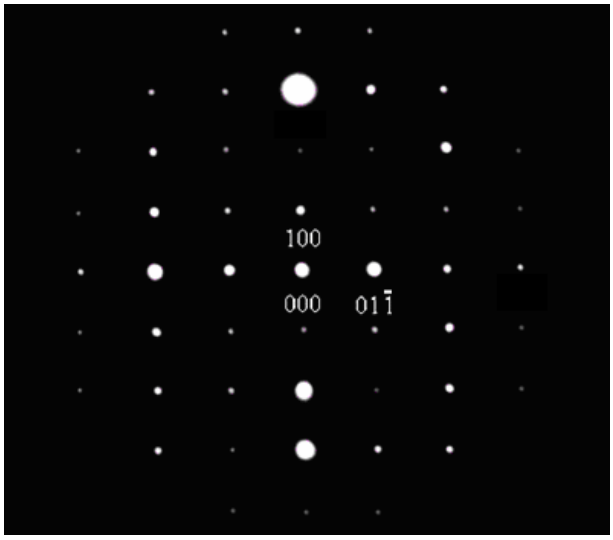

Fig. 7 (e)

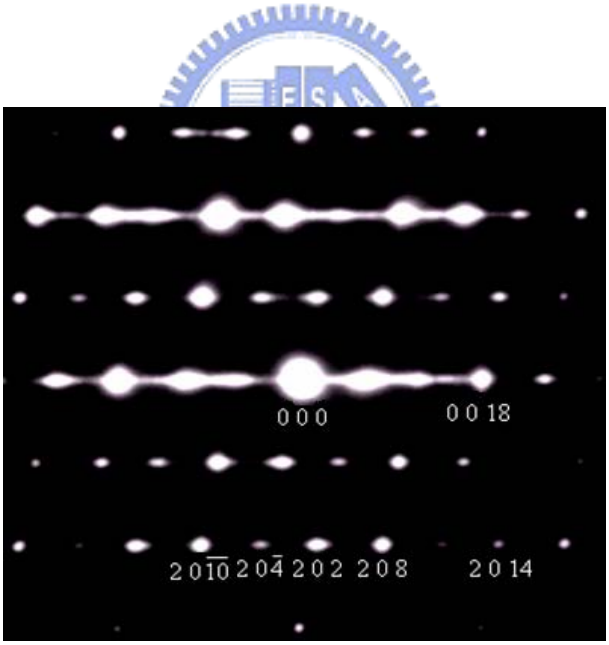

Fig. 7 (f)

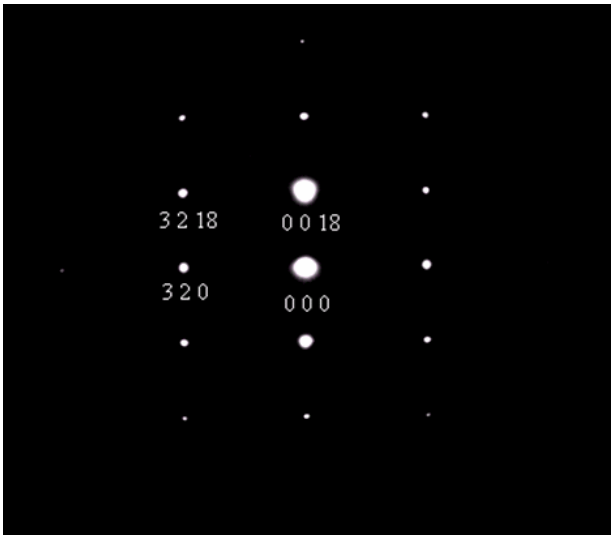

Fig. 7 (g)

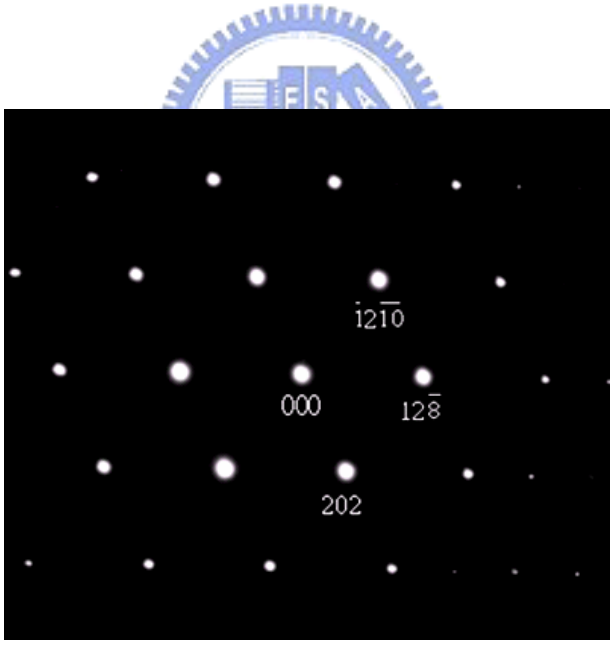

Fig. 7 (h)

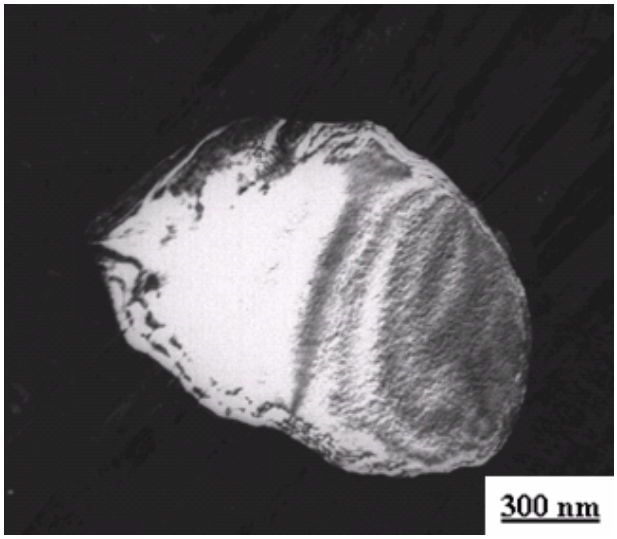

Fig. 7 (i)

Fig. 7 (a)-(b) Optical micrographs of the $Cu_{2.9}Mn_{0.1}Al$ alloy aged at 400℃ for (a) 1 hour and (b) 100 hours, respectively. (c)-(i) Electron micrographs of the $Cu_{2.9}Mn_{0.1}Al$ alloy aged at 400℃ for 100 hours (c)BF, (d)-(e) two SADPs taken from the precipitate marked as "R" in (c). The zone axes of the γ_2 phase are (d) [001] and (e)[011], respectively. (f)-(h) three SADPs taken from an area marked as "M" in (c). The zone axes of the β_1' martensite are (f) [010], (g) [230] and (h) $[\bar{2}92]$, respectively. (i) (100) γ_2 DF.

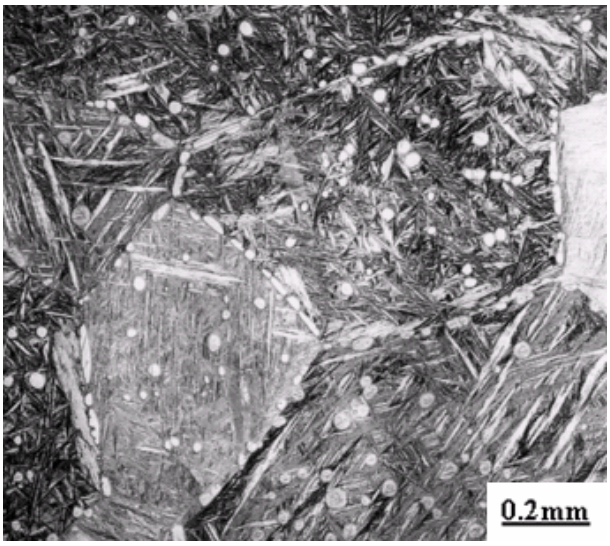

Fig. 8 (a)

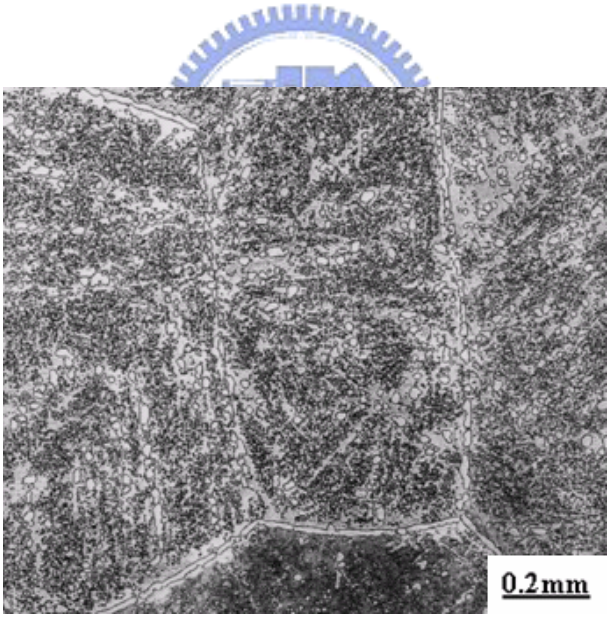

Fig. 8 (b)

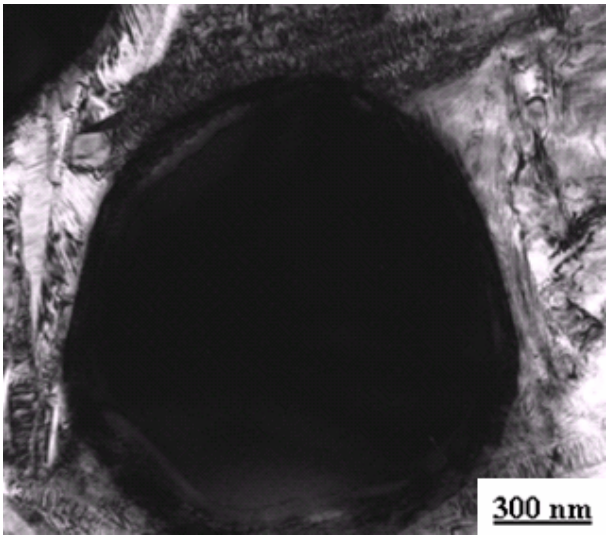

Fig. 8 (c)

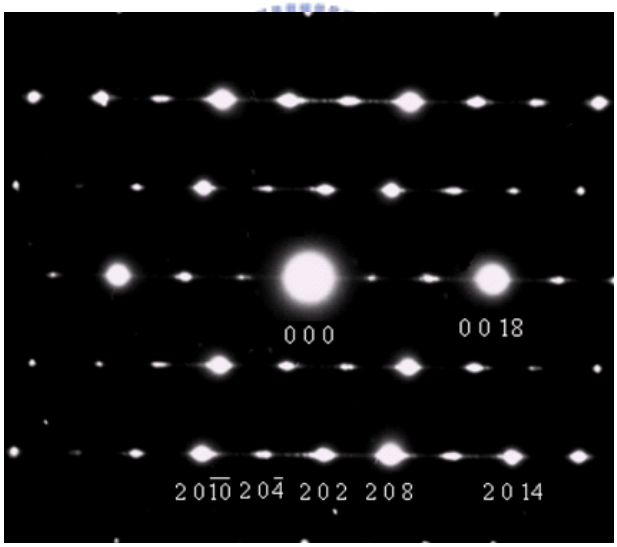

Fig. 8 (d)

Fig. 8 (a)-(b) Optical micrographs of the $Cu_{2.9}Mn_{0.1}Al$ alloy aged at 550℃ for (a) 1 hour and (b) 100 hours, respectively. (c)-(d) Electron micrographs: (c) BF, (d) a SADP of the β_1' martensite. The zone axis is [010].

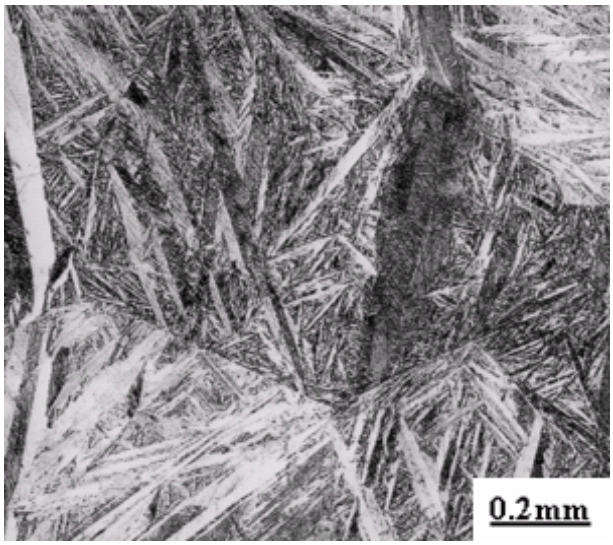

Fig. 9 (a)

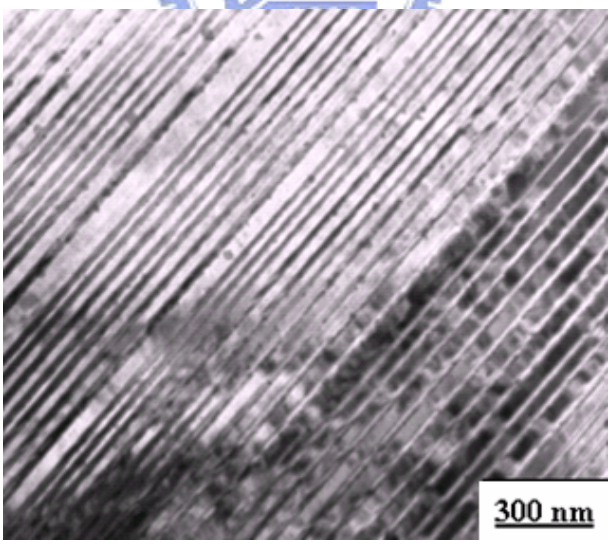

Fig. 9 (b)

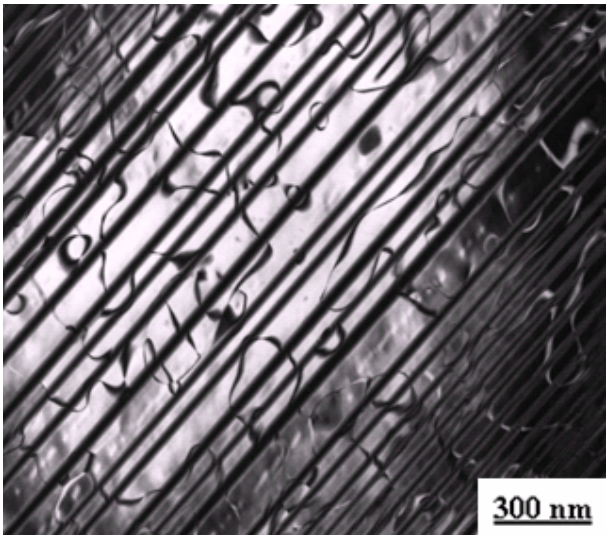

Fig. 9 (c)

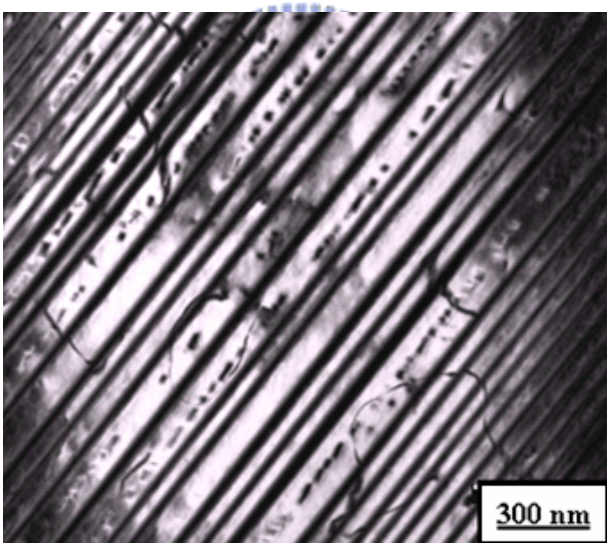

Fig. 9 (d)

Fig. 9 (a) Optical micrograph, (b)-(d) electron micrographs of the $Cu_{2.9}Mn_{0.1}Al$ alloy aged at 750℃ for 2 hours: (b) BF, (c) and (d) (111) and (200) $D0_3$ DF, respectively.

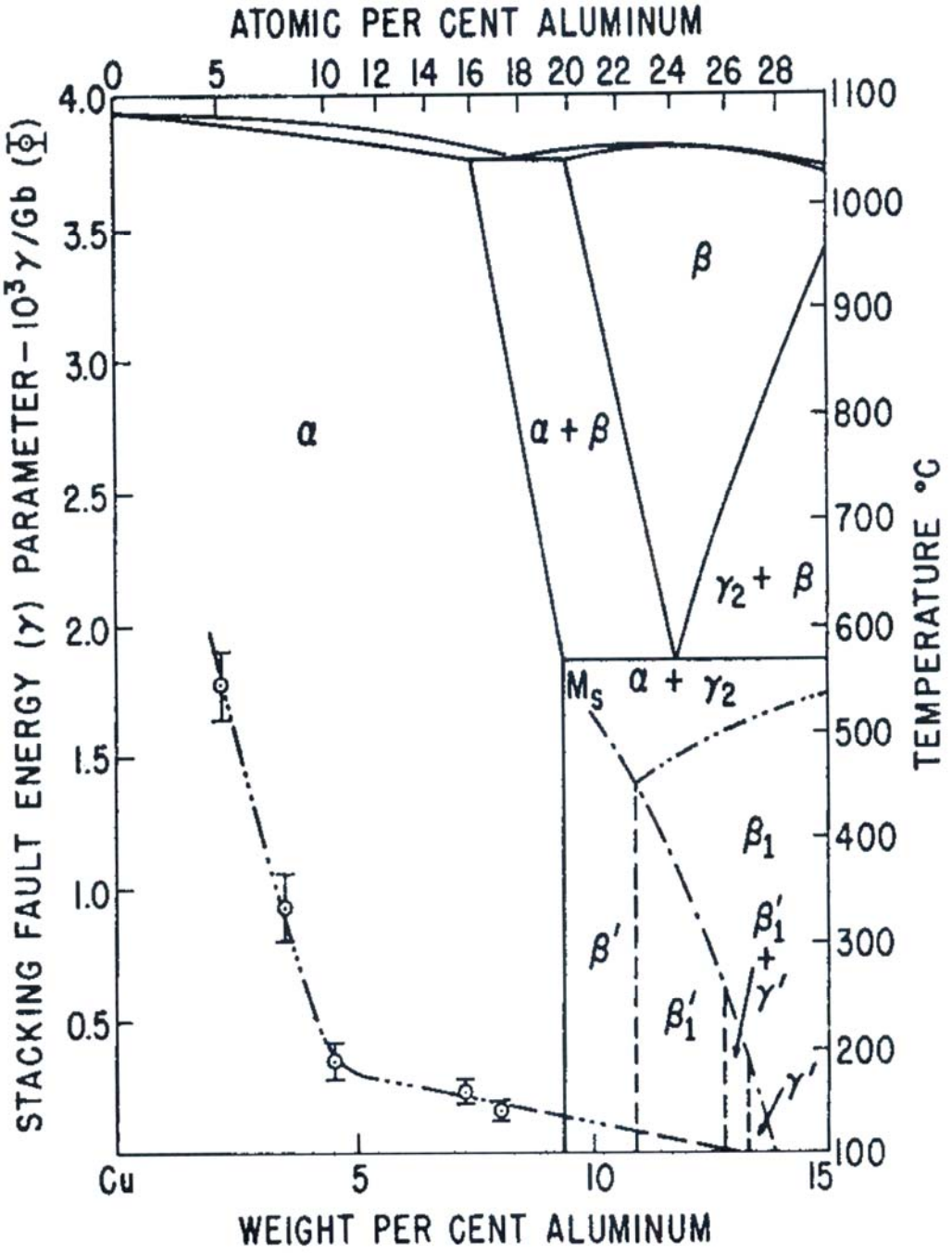

Fig. 10 A phase diagram containing metastable martensite phases in Cu-Al binary alloy system

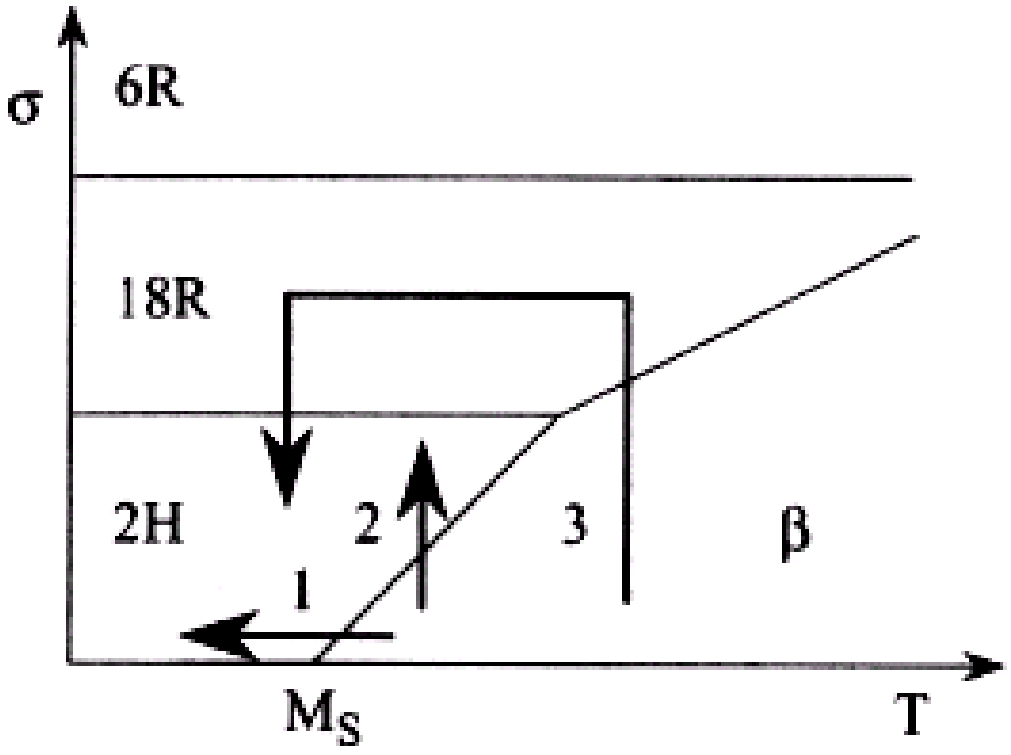

Fig. 11 A diagram of types of martensite with factors of temperature and stress

.